Bull Eng Geol Environ (2010) 69:111–118
DOI 10.1007/s10064-009-0220-3

ORIGINAL PAPER

Evaluation of the geology-environmental capacity of buildings based on the ANFIS model of the floor area ratio

Zhen-Dong Cui · Yi-Qun Tang · Xue-Xin Yan · Chun-Ling Yan · Han-Mei Wang · Jian-Xiu Wang

Received: 26 August 2008 / Accepted: 10 June 2009 / Published online: 11 July 2009

Abstract Land subsidence is a common geological hazard. The long-term accumulation of land subsidence in Shanghai has caused economic loss to the city. Since the 1990s, engineering structures have become a new cause of land subsidence. The concept of the geology-environmental capacity of buildings is put forward. The main factors involved in land subsidence were determined and related to the floor area ratio. The relationship was assessed using the adaptive neuro-fuzzy inference system for four typical regions in Shanghai, in order to give some guidance in respect of urban planning.

Keywords Geology-environmental capacity · Land subsidence · Floor area ratio · ANFIS

Introduction

Land subsidence is an environmental phenomenon resulting from consolidation of the ground. It is generally a relatively slow movement, but may break pipelines and result in differential settlement/tilting of buildings. The causes of land subsidence include natural factors (e.g. the collapsing of loess, drainage or organic-rich soils, karst development) and human activities (e.g. underground construction, removal of liquid and/or solids from the ground). In the coastal urban region of China, groundwater extraction is the primary cause of land subsidence (Chai et al. 2004, 2005; Gu 1998; Li et al. 2000).

In recent years, land subsidence has occurred in over 90 cities and counties in China, including Shanghai, Tianjin, Jiangsu Province, Shanxi Province; the total area of subsidence is reported as 93,885 km^2 (Cui 2008). Shanghai was one of the first cities to experience land subsidence. In the 80 years from 1921 to the end of 2001, the total accumulative subsidence had reached 2.7 m (Zhang and Wei 2002; Xue et al. 2005; Tang et al. 2008a). Initially, this was mainly due to the irrational withdrawal of groundwater but from the 1960s, the withdrawal of groundwater was restricted and from the end of the 1970s, the pumping of groundwater was strictly controlled in the urban area of Shanghai. As a consequence, the quantity of water recharged into the subsurface was always greater than that extracted by pumping, such that the subsidence caused by pumping and recharging was limited. During the 1990s, however, with the development of the economy, a variety of municipal works and high-rise buildings were constructed and land subsidence appeared to accelerate in Shanghai (Tang et al. 2008b; Cui et al. 2009).

In this paper, the "geology-environmental capacity" refers to the optimum inter-relationship between the needs of human society, the economy and the engineering structure in a certain geological area. The geology-environmental capacity is finite, e.g. there is a limit to the weight of the buildings that the ground can sustain in a certain geological situation if particular environmental criteria are to be met. In the soft soils of Shanghai, land subsidence caused by the engineering-environmental effect has resulted in great economic loss to the city, hence this has become an important factor, restricting the scale of

Z.-D. Cui (✉) · X.-X. Yan · H.-M. Wang
Shanghai Institute of Geological Survey, 200072 Shanghai, People's Republic of China
e-mail: czdjiaozuo@163.com

Z.-D. Cui · Y.-Q. Tang (✉) · C.-L. Yan · J.-X. Wang
Department of Geotechnical Engineering, Tongji University, 200092 Shanghai, People's Republic of China
e-mail: tangyiqu2@smail.tongji.edu.cn

construction. In Shanghai, therefore, building is mainly controlled by land subsidence.

Factors affecting land subsidence

Shanghai is situated on the Yangtze River delta where the alluvial deposits generally reach 250–300 m in the urban area (Fig. 1). The upper 150 m of the alluvium is mainly of grey, "soft-plastic" clay and sands. The lower horizon has a wider range of colours and is mainly "hard-plastic" clay alternating with layers of sand and gravel (Tang et al. 2008b).

In recent years, records indicate that the main subsidence below 70 m is related to pumping/recharge while the soil deformation above this depth was mainly caused by engineering works. In this upper horizon there are three distinct thick layers of soft soil, see Table 1.

Based on population density, engineering construction, hydraulic engineering, flood control etc., the area of Shanghai is divided into a basically stable region and a land subsidence region which contains two sub-regions as shown in Table 2.

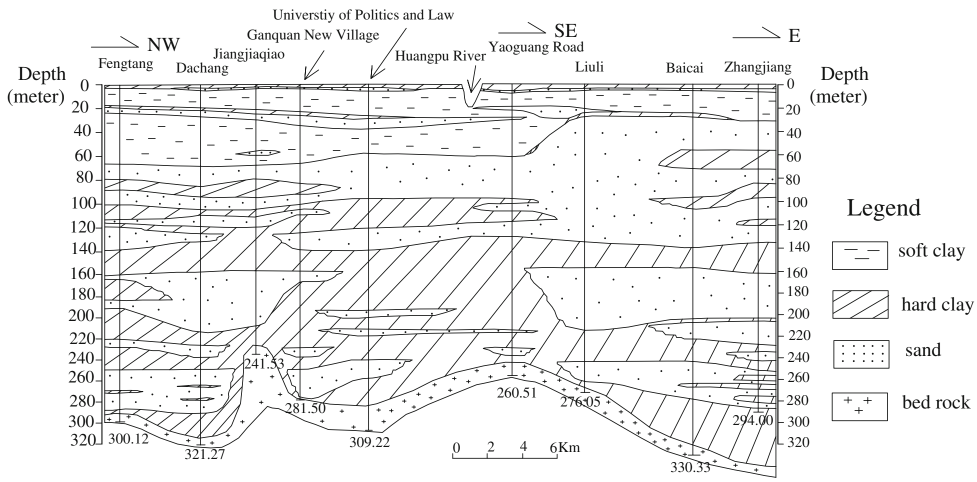

Fig. 1 Hydrostratigraphy along the cross section of Fengtang-Yaoguang Road-Zhangjiang

Table 1 Geological layers (above 70 m)

Engineering geology layer	The position of the aquifer	The depth of the roof	Thickness	Layer number	Second layer	Soil characteristics
Alluvium			0.00–7.00 m	I_1	I_1	Brown-yellow silty clay
No. 1 sand layer	Underwater	0.90–7.00 m	1.50–27.20 m	I_2	I_2	Grey silt with sandy silt
No. 1 hard soil		1.00–5.50 m	1.00–11.50 m	I_3	I_3	Brown-yellow, dark green clayey soil
No. 1 soft soil		About 3.00 m	12.00–20.00 m	I_4	I_4^1	Grey mucky silty clay with thin silt layer in-between
					I_4^2	Grey mucky clay
					I_5^1	Grey clay
No. 2 soft soil	Partially confined water	18.00–22.00 m	Several m ~30.00 m	I_5	I_5^2	Grey silty sand with sandy silt layer. Some gas
					I_5^3	Grey silty clay with silty marl in-between
No. 2 hard soil		15.00–30.0 m	2.00–12.60 m	II_1	II_1	Brown-yellow, dark green clayey soil
No. 2 sand layer	I	27.00–30.0 m	Several m ~20.00 m	II_2	II_2^1	Green-yellow silty fine sand with sandy silt
					II_2^2	Grey fine silty sand
No. 3 soft soil		25.00–50.0 m	Several m ~35.00 m	II_3	II_3^1	Grey silty clay with silty and fine sand
					II_3^2	Grey silty clay and silty sand
					II_4^1	Grey fine sand with gravel
No. 3 sand layer	II	45.00–60.00 m	30.00–50.00 m	II_4		Grey, grey-green and putty color mucky soil
					II_4^2	Light grey fine sand with gravel

Table 2 Distribution of land subsidence in Shanghai

Region	Sub-region	Distribution range	Area (km^2)	Land subsidence	Subsidence
Basic stability region		Qingpu District, Songjiang District, Jinshan District	353.34	The accumulation of land subsidence is not over 25 mm from 1980 to 1995 and the annual average subsidence is less than 1.7 mm/a	Not seen
Land subsidence region	Subsidence sub-region	Pudong New District, Baoshan District, Minhang District, Jiading District, Fengxian District, Nanhui District, Songjiang District, Jinshan District, Qingpu District, Chongming County	5736.66	The accumulation of land subsidence is 25–100 mm from 1980 to 1995 and the annual average subsidence is 1.7–6.7 mm/a	The disaster is not obvious
	Subsidence sub-region	Urban, suburb	250.5	The accumulation of land subsidence is over 100 mm from 1980 to 1995 and the annual average subsidence is over 6.7 mm/a	The disaster is more obvious

Table 3 Building area of four typical regions (Unit: $\times 10^6$ m^2)

Region	Before 1970s	Increase in area in 1970s	Increase in area in 1980s	Increase in area in 1990s	Total area
Lujiazui	5.24	0.80	1.57	3.94	11.55
Xujiahui	6.80	0.72	1.75	2.30	11.57
Zhongyuan	3.47	0.51	1.57	2.78	8.33
Changqiao	2.85	0.20	1.31	2.31	6.67
Total area	18.36	2.23	6.20	11.33	38.12

Density of construction

The floor area ratio is the ratio of the total floor area within an individual structure to the area of land on which the construction has taken place. The building density is the ratio of the basement area of the building to the area of land on which the construction has taken place.

As shown in Table 3 (Yan et al. 2002) the building areas of four typical regions, Lujiazui, Xujiahui, Zhongyuan and Changqiao increased from 1980 to 1999. It can be seen that the built area increased in the 1980s and 1990s relative to that in the previous decade. In most areas, the floor space more than doubled. In the same period, land subsidence increased rapidly (Table 4), again more than doubling between the 1980s and 1990s.

Table 5 indicates the number of high rise buildings constructed in the four areas together with the total floor areas. The value of the floor area ratio is derived from the proportion of the number of the high-rise buildings to the total number of buildings.

Table 4 Land subsidence of four typical regions (Unit: mm)

Region	In 1970s	In 1980s	In 1990s
Lujiazui	−0.30	−3.52	−12.56
Xujiahui	−2.13	−3.16	−7.18
Zhongyuan	−1.37	−4.49	−15.14
Changqiao	−0.89	−2.92	−7.95

The adaptive neuro-fuzzy inference system

The adaptive neuro-fuzzy inference system (ANFIS) combines artificial neural networks (Mamdani and Assilian 1975; Jacobs 1988; Hoke and Brown 1997) with the (Sugeno) fuzzy logic inference. The typical fuzzy logic rule is as follows.

If x is A and y is B, then $Z = f(x, y)$, where A and B are the fuzzy set of the inputs and $z = f(x, y)$ is the accurate function of the target. Generally, $f(x,y)$ is polynomial about input variables x, y. If $f(x, y)$ is one-order polynomial, the

Table 5 The floor area ratio of four typical regions

Region	Total building area ($\times 10^6$ m^2)	Building area of high-rise building ($\times 10^6$ m^2)	Number of high-rise buildings	The ratio of high-rise buildings to total buildings (%)	Land area ($\times 10^6$m^2)	The floor area ratio
Lujiazui	11.17	3.58	123	32.01	7.37	1.53
Xujiahui	9.79	2.33	126	23.77	6.98	1.40
Zhongyuan	8.09	0.57	47	57.25	6.88	1.18
Changqiao	6.17	0.42	36	42.34	6.89	0.90

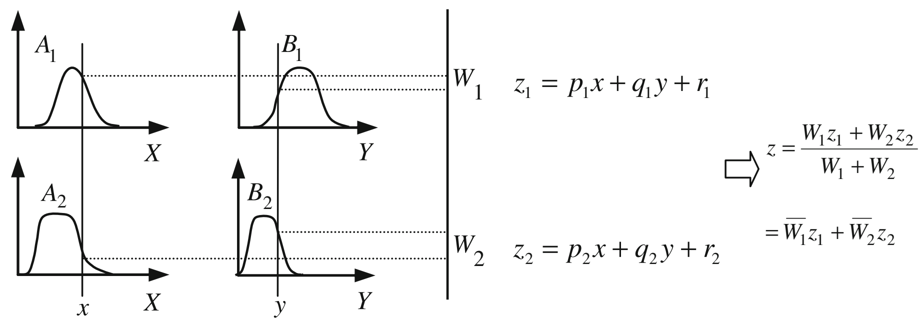

Fig. 2 The inference process of one-order Sugeno fuzzy system

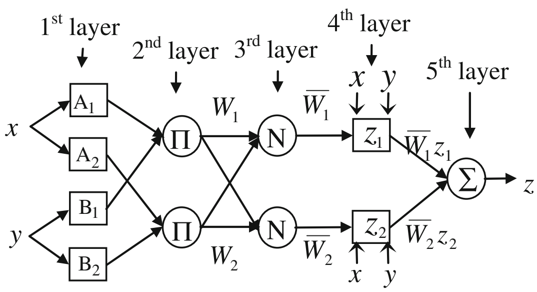

Fig. 3 The ANFIS structure equivalent to one-order Sugeno

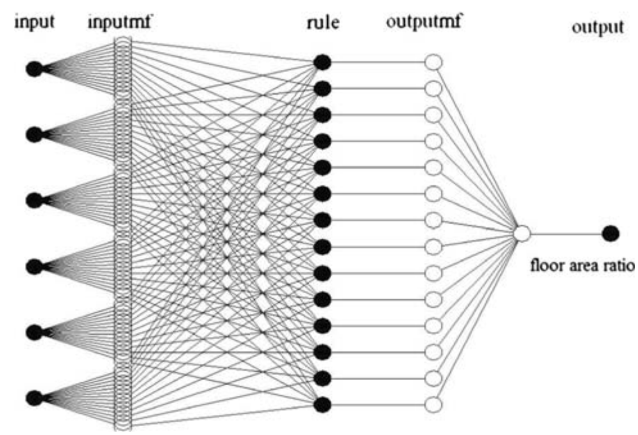

Fig. 4 The structure of ANFIS

Table 6 ANFIS training data

	S	D	C	K	H	J	R
1	150	0.296	100	3,166.7650	184.3086	100	7.86
2	100	0.301	70	4,168.9943	240.2756	50	5.62
3	60	0.260	40	4,562.6321	216.7324	50	1.5
4	85	0.274	70	3,213.4352	192.1249	50	2.0
5	90	0.267	70	4,316.2984	209.3765	50	2.0
6	120	0.288	100	3,200.2712	196.0024	100	4.78
7	95	0.320	100	457.8083	763.2687	60	3.90
8	60	0.315	100	586.4392	999.9386	60	2.0
9	120	0.302	100	578.4218	999.7294	60	1.5
10	140	0.321	100	573.2672	889.8367	60	2.0
11	105	0.330	100	590.3024	1001.2626	60	1.5
12	30	0.320	100	19.1032	16.2270	80	1.5
13	40	0.332	100	22.6857	30.7264	80	2.0
14	35	0.331	100	27.6858	33.0413	80	2.0
15	25	0.317	100	28.1023	32.7869	80	1.5
16	30	0.343	100	26.7474	32.976	80	4.3
17	40	0.284	40	1,709.3189	10.8912	50	1.0
18	50	0.293	40	1,379.2179	5.1610	50	1.5
19	45	0.302	40	936.3198	3.0826	50	2.0

obtained fuzzy inference system is the one-order Sugeno fuzzy model.

Figure 2 shows the inference process of the one-order Sugeno fuzzy model which has two inputs x, y and one output z, such that it contains two fuzzy "if-then" rules:

If x is A_1 and y is B_1, then $f_1 = p_1x + q_1y + r_1$.

If x is A_2 and y is B_2, then $f_2 = p_2x + q_2y + r_2$.

where A_i and B_i are fuzzy sets corresponding with input variables.

Supposing that the S type membership functions of input variables x and y are:

$$S_{A_i}(x, a_i, b_i) = \frac{1}{1 + e^{-a_i(x-b_i)}} \tag{1}$$

$$S_{B_i}(y, c_i, d_i) = \frac{1}{1 + e^{-c_i(x-d_i)}} \tag{2}$$

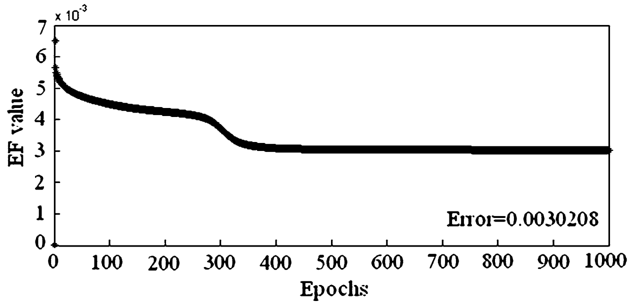

Fig. 5 The training error in the training process

where $i = 1, 2$ $\{a_i, b_i\}$ and $\{c_i, d_i\}$ being two group characteristic parameters of S type membership functions.

S type membership functions are changed with the change of the values of characteristic parameters, that is, the membership functions of A_i and B_i are changed. The inference process can be equivalent to the ANFIS structure shown in Fig. 3 which consists of five layers.

The function of the first layer is to compute the fuzzy membership of inputs. Every node of this layer is the adaptive node and has a node function,

$$O_{1,i} = S_{A_i}(x, a_i, b_i), \quad i = 1, 2 \tag{3}$$

$$O_{1,j} = S_{B_{j-2}}(y, c_{j-2}, d_{j-2}), \quad j = 3, 4 \tag{4}$$

where $O_{1,i}$ is the No.i output of the first layer and is a member of the corresponding output variable of fuzzy sets A_i and B_i

The function of the second layer is to compute the fitness of every rule. Every node of this layer is a fixed node labeled $\prod$. Its output is the product of all input signals:

$$O_{2,1} = O_{1,1} \cdot O_{1,3} = S_{A_1}(x, a_1, b_1) \cdot S_{B_1}(y, c_1, d_1), \text{marking } W_1 \tag{5}$$

$$O_{2,2} = O_{1,2} \cdot O_{1,4} = S_{A_2}(x, a_2, b_2) \cdot S_{B_2}(y, c_2, d_2), \text{marking } W_2 \tag{6}$$

The function of the third layer is to compute the unitary value of fitness. Every node of this layer is a fixed node labeled *N*. The ratio of the strength of one rule to the sum of all the strengths is obtained:

$$O_{3,1} = \bar{W}_1 = \frac{W_1}{W_1 + W_2} \tag{7}$$

$$O_{3,2} = \bar{W}_2 = \frac{W_2}{W_1 + W_2} \tag{8}$$

Fig. 6 The membership function of land subsidence before and after training

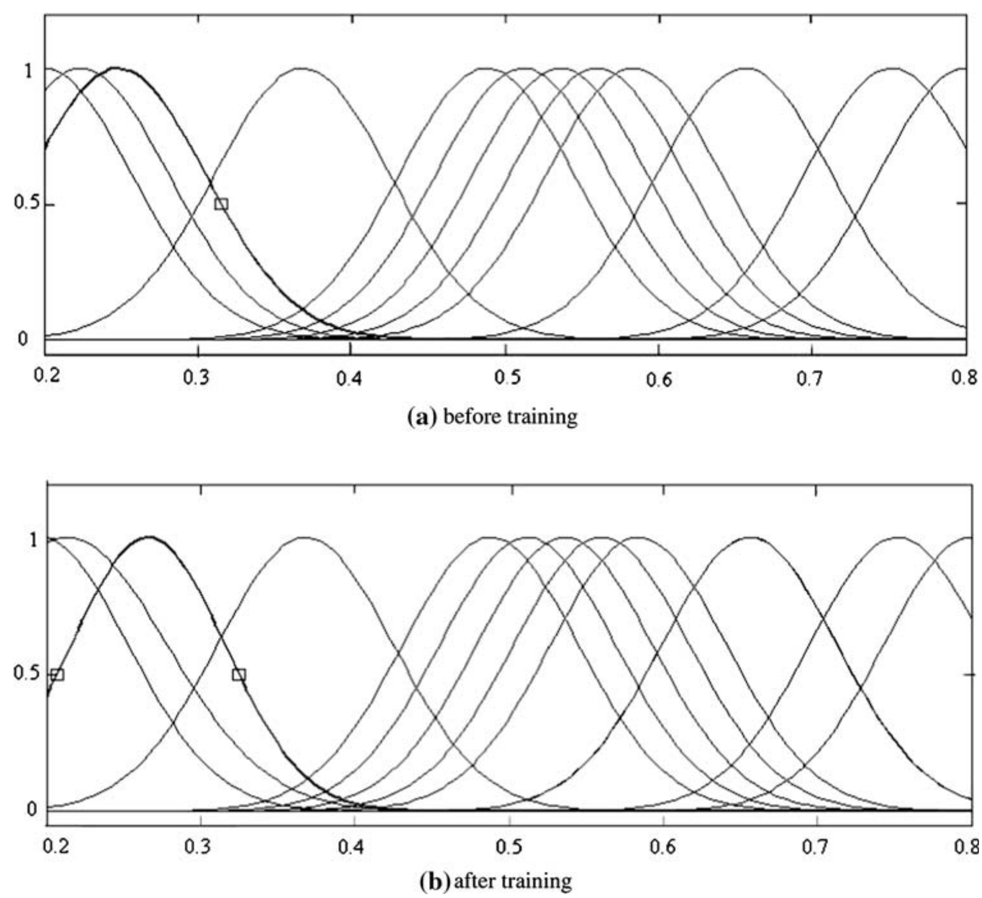

The function of the fourth layer is to compute the output of every rule. Every node of this layer is an adaptive node with a function:

$$O_{4,1} = \bar{W}_1 z_1 = \bar{W}_1(p_1 x + q_1 y + r_1) \quad (9)$$

$$O_{4,2} = \bar{W}_2 z_2 = \bar{W}_2(p_2 x + q_2 y + r_2) \quad (10)$$

where $\{p_i,\ q_i,\ r_i\}$ $(i = 1,\ 2)$ is the set of parameters of corresponding nodes, i.e. conclusion parameters.

The function of the fifth layer is to compute the output of the fuzzy system. The single node of this layer is a fixed node ($\sum$) which computes the sum of all the incoming signals:

$$O_5 = z = \sum \bar{W}_i z_i = \bar{W}_1 z_1 + \bar{W}_2 z_2 \quad (11)$$

This network consists of undetermined characteristic parameters (a_i, b_i, c_i, d_i $(i = 1, 2)$ of membership functions and p_i, q_i, r_i $(i = 1,\ 2)$ conclusion parameters). ANFIS dynamically adjusts these parameters in the trained process.

ANFIS model based on the floor area ratio

Land subsidence S, the building density D, the geological disaster district C, the exploitation of groundwater K, the re-circulation of groundwater H and the type of the geology structure J were selected as the variables to infer the floor area ratio R in this paper, that is, $X = (S,\ D,\ C,\ K,\ H,\ J)$. The relationship between R and X is,

$$R = F(\{X\}) \quad (12)$$

This can be established using ANFIS as follows.

(1) The finite groups of the training data are obtained at different places according to the influencing factor X and the floor area ratio R.
(2) X and R are taken as the input data and the output data of the initial structure of ANFIS, respectively. After training, the optimum structure model of ANFIS reflecting the global mapping relationship is built up between X and R.
(3) Putting the data of four typical regions into this structure model of ANFIS, the output is the predicted optimum value of the floor area ratio.

Nineteen examples were selected as the training data, from different places in Shanghai; the variables are shown

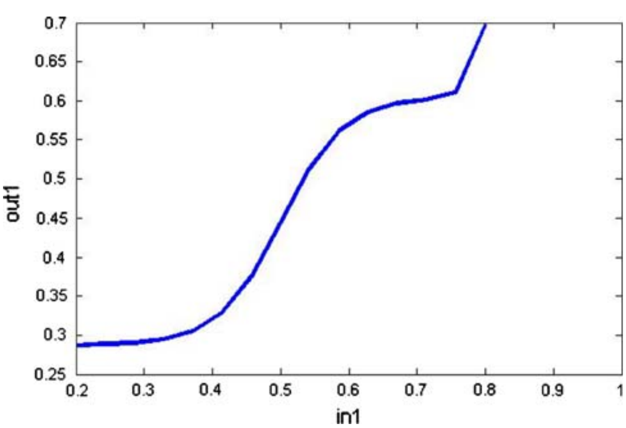

Fig. 7 The changing law between S and R

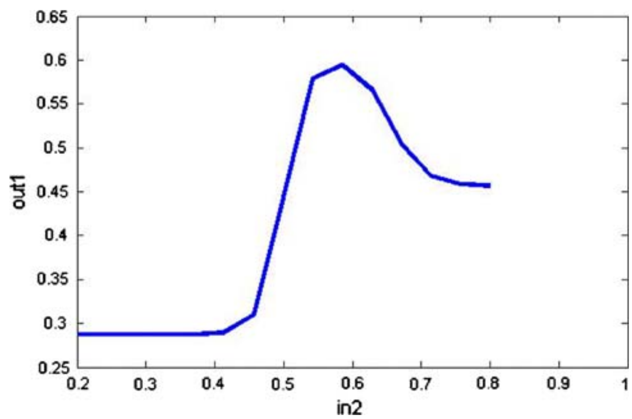

Fig. 8 The changing law between D and R

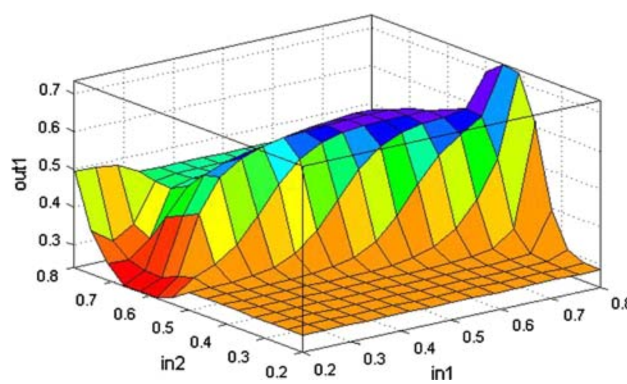

Fig. 9 The changing law between S, D and R

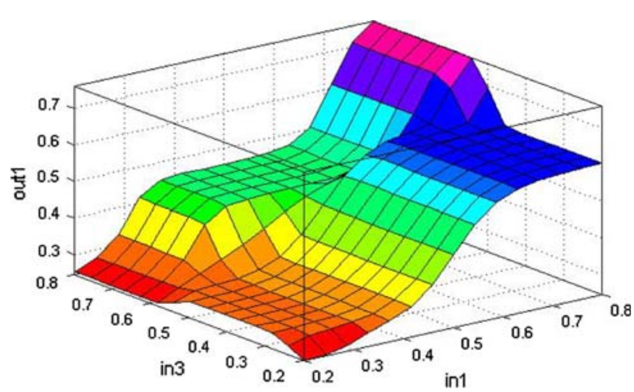

Fig. 10 The changing law between S, C and R

in Table 6. The variables of the 16 examples in Table 6 were treated in the standardized way. The *S*, *D*, *C*, *K*, *H* and *J* are the input of the network and the *R* is the output of the network. A model structure was built up by the subtraction cluster method. The values of the training parameters were

Range of influence 0.27, Squash factor 1.25,

Accept ratio 0.5, Reject ratio 0.15.

Every input variable of the model was automatically endowed with 16 Gauss membership functions. The model structure based on the floor area ratio is shown in Fig. 4. Using the hybrid learning algorithm, the network was trained by the selected data. The training degree was 1,000 times and the smallest root-mean-square deviation of the training data was 0.0030208. The change of the error in the training process is shown in Fig. 5.

The membership functions of land subsidence *S*, the building density *D*, the geological disaster district *C*, the exploitation of groundwater *K*, the re-circulation of groundwater *H* and the type of the geology structure *J* can be obtained before and after training. The membership function of land subsidence as an example is shown in Fig. 6.

Six pictures of the changing laws between one single input parameter of *S*, *D*, *C*, *K*, *H*, *J* and the output parameter *R* can be obtained. The changing laws of *S*-*R* and *D*-*R* as two examples are shown in Figs. 7 and 8. Fifteen pictures of the changing laws between every two input parameters of *S*, *D*, C, *K*, *H*, *J* and the output parameter *R* can also be obtained. The changing laws of *S*, *D*-*R* and *S*, *C*-*R* as two examples are shown in Figs. 9 and 10.

Evaluation of the geology-environmental capacity of the buildings based on the ANFIS model of the floor area ratios are shown in Figs. 11, 12, 13 and 14. Where the floor area ratios of the regions are bigger, the high-rise buildings are dense and land subsidence is larger. It is inappropriate to continue to plan high-rise construction in these regions. However, where the floor area ratios of the regions are smaller and land subsidence is less, high-rise buildings can be constructed.

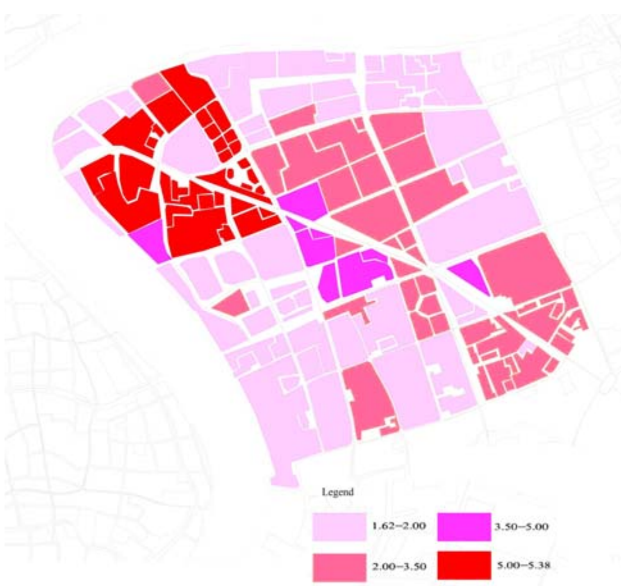

Fig. 11 The floor area ratios of the 1st typical region

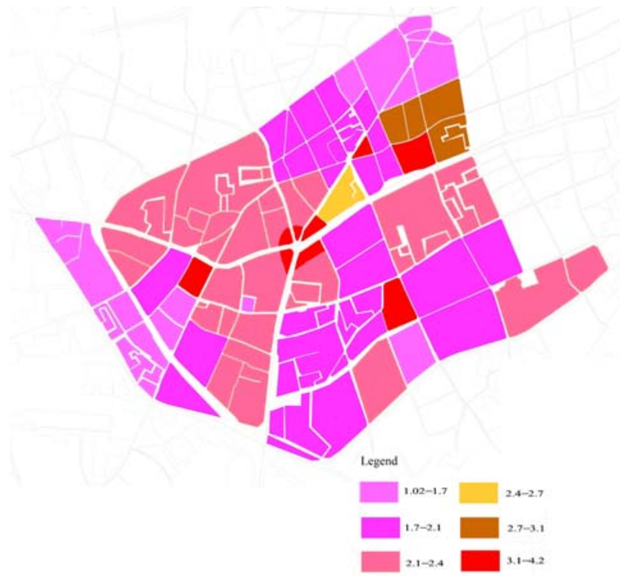

Fig. 12 The floor area ratios of the 2nd typical region

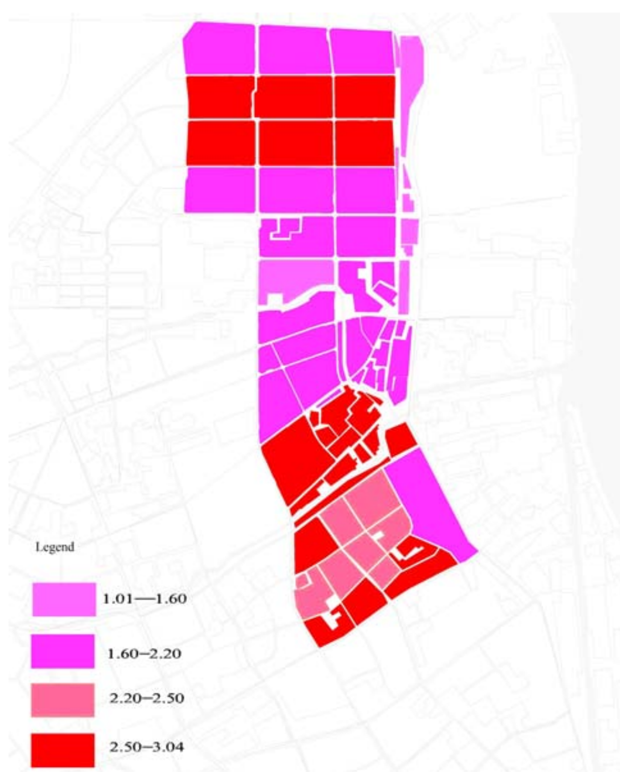

Fig. 13 The floor area ratios of the 3rd typical region

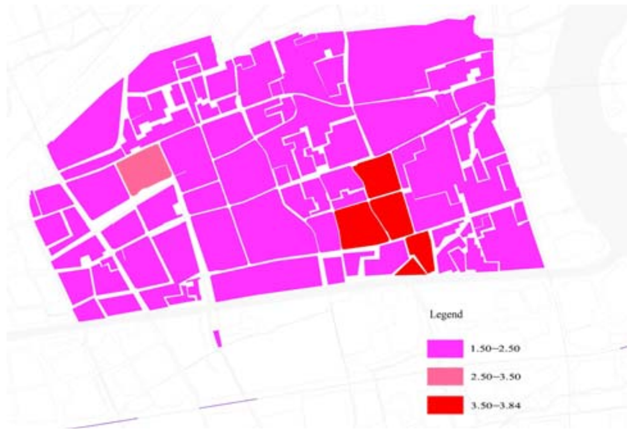

Fig. 14 The floor area ratios of the 4th typical region

Conclusions

The paper has demonstrated that as the geological environmental capacity of a building is mainly controlled by the land subsidence in the Shanghi area, the relationship can be assessed using the floor area ratio. ANFIS was used to evaluate the floor area ratios of four typical areas in the Shanghai region (Lujiazui, Xujiahui, Zhongyuan and Changqiao) in order to offer some guidance in respect of urban planning.

Acknowledgments The work presented in this paper was supported by a research grant from the Ministry of Land and Resources of China and the Shanghai Municipal Government.

References

Chai JC, Shen SL, Zhu HH, Zhang XL (2004) Land subsidence due to groundwater drawdown in Shanghai. Geotechnique 54(3):143–148

Chai JC, Shen SL, Zhu HH, Zhang XL (2005) 1D analysis of land subsidence in Shanghai. Lowland Technol Int 7(1):33–41

Cui ZD (2008) Study of land subsidence caused by the dense high-rise building group in the soft soil area (in Chinese). Tongji University, Shanghai

Cui ZD, Tang YQ, Yan XX (2009) Centrifuge modeling of land subsidence caused by the high-rise building group in the soft soil area. Environ Earth Sci. doi: 10.1007/s12665-009-0163-9

Gu XY (1998) Review and prospects of land subsidence computation (in Chinese). Chin J Geolog Hazard Control 93(2):81–85

Hoke E, Brown ET (1997) Practical estimates of rock mass strength. Int J Rock Mech Min Sci G Abstr 34(8):106–119

Jacobs RA (1988) Increased rates of convergence through learning rate adaptation. Neural Netw 17(1):295–307

Li QF, Fang Z, Wang HM (2000) A mathematical model and forecast of groundwater workable reserves for Shanghai (in Chinese). Shanghai Geol 23(2):36–43

Mamdani EH, Assilian S (1975) An experiment in linguistic synthesis with a fuzzy logic controller. Int J Man Mach Stud 7(1):1–13

Tang YQ, Cui ZD, Wang JX, Yan LP, Yan XX (2008a) Application of grey theory-based model to prediction of land subsidence due to engineering environment in Shanghai. Environ Geol 55(3):583–593

Tang YQ, Cui ZD, Wang JX, Lu C, Yan XX (2008b) Model test study of land subsidence caused by the high-rise building group. Bull Eng Geol Environ 67(2):173–179

Xue YQ, Zhang Y, Ye SJ Wu JC, Li QF (2005) Land subsidence in China. Environ Geol 48:713–720

Yan XX, Gong SL, Zeng Z (2002) Relationship between building density and land subsidence in Shanghai urban zone (in Chinese). Hydrogeol Eng Geol 33(6):21–26

Zhang AG, Wei ZX (2002) Past, present and future research on land subsidence in Shanghai (in Chinese). Hydrogeol Eng Geol 33(5):72–75